

# ALX4 dysfunction disrupts craniofacial and epidermal development

Hulya Kayserili<sup>1,†</sup>, Elif Uz<sup>2,3,†</sup>, Carien Niessen<sup>6,7,9</sup>, Ibrahim Vargel<sup>4,11</sup>, Yasemin Alanay<sup>5</sup>, Gokhan Tuncbilek<sup>4</sup>, Gokhan Yigit<sup>7,8</sup>, Oya Uyguner<sup>1</sup>, Sukru Candan<sup>1</sup>, Hamza Okur<sup>3</sup>, Serkan Kaygin<sup>10</sup>, Sevim Balci<sup>5</sup>, Emin Mavili<sup>4</sup>, Mehmet Alikasifoglu<sup>2,5</sup>, Ingo Haase<sup>6,7,9</sup>, Bernd Wollnik<sup>7,8,9,\*</sup> and Nurten Ayse Akarsu<sup>2,3,\*</sup>†

<sup>1</sup>Department of Medical Genetics, Istanbul Medical Faculty, Istanbul University, Istanbul 34094, Turkey, <sup>2</sup>Department of Medical Genetics, <sup>3</sup>Gene Mapping Laboratory, Pediatric Hematology Unit, <sup>4</sup>Department of Plastic and Reconstructive Surgery and <sup>5</sup>Genetics Unit, Department of Pediatrics, Hacettepe University, Medical Faculty, Ankara 06100, Turkey, <sup>6</sup>Department of Dermatology, <sup>7</sup>Center for Molecular Medicine Cologne (CMMC), <sup>8</sup>Institute of Human Genetics and <sup>9</sup>Cologne Excellence Cluster on Cellular Stress Responses in Aging-Associated Diseases (CECAD), University of Cologne, Cologne 50931, Germany, <sup>10</sup>Hemosoft, Inc., Ankara 06100, Turkey and <sup>11</sup>Department of Plastic and Reconstructive Surgery, Kirikkale University, Medical Faculty, Kirikkale 71000, Turkey

Received April 13, 2009; Revised August 7, 2009; Accepted August 13, 2009

**Genetic control of craniofacial morphogenesis requires a complex interaction of numerous genes encoding factors essential for patterning and differentiation. We present two Turkish families with a new autosomal recessive frontofacial dysostosis syndrome characterized by total alopecia, a large skull defect, coronal craniosynostosis, hypertelorism, severely depressed nasal bridge and ridge, bifid nasal tip, hypogonadism, callosal body agenesis and mental retardation. Using homozygosity mapping, we mapped the entity to chromosome 11p11.2–q12.3 and subsequently identified a homozygous c.793C→T nonsense mutation in the human ortholog of the mouse *aristaless*-like homeobox 4 (*ALX4*) gene. This mutation is predicted to result in a premature stop codon (p.R265X) of *ALX4* truncating 146 amino acids of the protein including a part of the highly conserved homeodomain and the C-terminal paired tail domain. Although the RNA is stable and not degraded by nonsense-mediated RNA decay, the mutant protein is likely to be non-functional. In a skin biopsy of an affected individual, we observed a hypomorphic interfollicular epidermis with reduced suprabasal layers associated with impaired interfollicular epidermal differentiation. Hair follicle-like structures were present but showed altered differentiation. Our data indicate that *ALX4* plays a critical role both in craniofacial development as in skin and hair follicle development in human.**

## INTRODUCTION

Facial development in vertebrates is a dynamic and complex process that originates from several primordia, especially during the fourth and fifth week of embryonic development. Primordia consist of an unpaired frontonasal prominence and paired nasomedial, maxillary and mandibular processes (1). The frontonasal prominence mainly derives from mesenchy-

mal neural crest cells bordered by epithelia from the forebrain and facial ectoderm. The outgrowth of the facial primordia depends on mesenchymal–ectodermal interactions, which are in part controlled by the overlying epithelium (2). Genetic control of facial morphogenesis requires an integrated action of various genes encoding factors essential for patterning and differentiation, such as transcription factors and signaling molecules (3). Alterations in this network that cause

\*To whom correspondence should be addressed at: Department of Medical Genetics, Hacettepe University Medical Faculty, Sıhhiye, Ankara 06100, Turkey. Tel: +90 3123052559 (N.A.A.)/+49 22147886817 (B.W.); Fax: +90 3124268592 (N.A.A.)/+49 22147886812 (B.W.); Email: nakarsu@hacettepe.edu.tr (N.A.A.) or bwollnik@uni-koeln.de (B.W.)

†The authors wish it to be known that, in their opinion, the first two and the last two authors should be regarded as joint Authors.

dysfunctional signaling and disturbed mesenchyme–epithelial interactions, can result in a number of frontofacionasal malformations and various degrees of facial clefting.

The nosology of human facial malformation syndromes is complex. The Online Mendelian Inheritance in Man catalogue (OMIM) lists more than 100 entries which show median clefting, frontonasal dysplasia/dysostosis and bifid nose. Frontonasal dysplasia (or frontonasal dysostosis, FND; OMIM 136760) is a commonly used term to describe abnormal median facial development characterized by an incomplete migration of the orbits into their proper position, resulting in widely separated eyes or hypertelorism (4,5). Such incomplete medial migration may show additionally in anterior cranium bifidum, midline clefts of the nose, lip, palate and forehead. The spectrum of abnormal face development in the various entities showing FND is wide (6–8). The etiology of FND is largely unknown. Mutations in a ligand of the ephrin receptor tyrosine kinases (*EFNB1*) detected in patients with craniofrontonasal syndrome [CFNS (OMIM 304110)], represent the thus far only known genetic cause for FND (9,10).

Here, we report a new frontonasal dysplasia phenotype associated with alopecia and hypogonadism in two consanguineous families from Turkey. We mapped the locus for this entity to chromosome 11p11.2–q12.3 and identified a homozygous nonsense mutation in the human aristaless like 4 (*ALX4*) gene in both families. The mutation is predicted to cause a truncation of the *ALX4* protein affecting the important homeodomain. Molecular, histological and immunohistological studies indicate that *ALX4* plays a critical role in craniofacial development, skin structure and proper hair follicle development in human.

## RESULTS

### Clinical characteristics

The parents of all affected individuals in the two families were consanguineous (Fig. 1A–I) and both families originated from two nearby cities in the Black Sea region of Turkey suggesting a founder effect. No link between the two families could be detected; however, symptoms in affected individuals were very similar.

**Family 1.** The index patient (Fig. 1G, individual IV-1) was born after a 32-week pregnancy complicated by intrauterine growth retardation and oligohydramnios. Sonography at 30 weeks had shown unclassifiable facial abnormalities. At birth his weight was 1100 g (–2.4 SDS), height was 33 cm (–2.1 SDS) and occipitofrontal circumference was 27 cm (–2.1 SDS). Clinical evaluation at 8 weeks showed total alopecia, brachycephaly, a skull defect over the sagittal suture, prominent forehead, marked hypertelorism, telecanthi, blepharophimosis, microphthalmia, strabismus and horizontal nystagmus, broad nasal bridge and ridge, bifid and depressed nasal tip, broad columella, anteverted nares, notched alae nasi, broad philtrum, and low-set ears with large lobules that were uplifted (Fig. 1A and B). Intra-oral structures were normal. His scrotum was underdeveloped and there was bilateral cryptorchidism. Three-dimensional computed tomography scan (3D-CT scan) demonstrated a cranium bifidum increased distance between orbits, coronal synostosis, aplasia of ethmoid

and nasal bones and underdevelopment of the maxillary bones (Fig. 1C). He was able to stand at 16 months and walked independently at 2 years of age, although only unsteady. His developmental level at 36 months (Denver II scale) showed a developmental age of 20–27 months, although his fine motor skills were more retarded due to his vision problems. At 3 years, he had sparse and thin hair at the occipital region but otherwise facial features had remained unchanged. Echography of heart and abdomen and a skeletal survey gave normal results. Eye examination showed bilateral microphthalmia and vertical nystagmus. Chromosome analysis (600 bands) showed a normal male karyotype. Cranial magnetic resonance imaging (MRI) showed agenesis of the inferior cerebellar vermis, and agenesis of the rostrum and splenium of corpus callosum. In addition, a 2 × 1 cm mass, hyperintense on T1W sequence and suggestive of a lipoma, was detected adjacent to the corpus callosum.

Clinical evaluation of the parents showed no abnormalities in mother and macrocephaly in father [OFC 60.5 cm (3.8 SDS)] with bilateral small skull defects aside the midline of the occiput. 3D cranial CT scan confirmed the presence of parietal foramina (Fig. 1I).

**Family 2.** No reliable data were available for the index patient (Fig. 1H; IV-8) in the first year of life. The case was considered compatible with bilateral Tessier 1–13 cleft according to the Tessier clefting system (11,12). Orbital medialization and frontal defect repair with calvarial allografts were performed at 5 years of age. He had mild to moderate developmental delay (walking at 4 years; three word sentences at 6 years). On physical exam at 8 years of age, he had total alopecia, brachycephaly, microcephaly [head circumference 48 cm (–2 SDS)], skull defects, hypertelorism, telecanthi, broad nasal bridge and ridge, bifid and depressed nasal tip, anteverted nares, notched alae, broad philtrum, widely spaced, conical teeth and large ear lobules (Fig. 1D and E). Ophthalmological examination showed blepharophimosis, strabismus and a rotatory nystagmus. Several small naevi on the occipital region of scalp were noted (Fig. 1F, upper part). There was bilateral cryptorchidism. At that age, and also later on, he lacked almost all body hair. Cranial 3D-CT scan (Fig. 1F, bottom part) and cranial MRI showed large calvarial bone defects, coronal synostosis, underdeveloped maxillary bones and absent nasal bones, and a lipoma in the splenium of corpus callosum. At age 19, he was seen prior to reconstructive surgery for repair of alar clefts. He was literate and had a friendly personality. Both parents had normal skull shapes and facial features. They have had an earlier son who was stated to have a very similar phenotype and died at 2 months of age because of respiratory difficulty (Fig. 1H; IV-7). Furthermore, family history showed another relative at 40 years of age (Fig. 1H; IV-1) with a similar phenotype, who was not available for clinical evaluation.

### Homozygosity mapping and identification of a causative *ALX4* mutation

Initially, we excluded *EFNB1* gene mutations in our families by direct sequencing of all coding exons (data not shown). Available affected individuals and parents were typed using

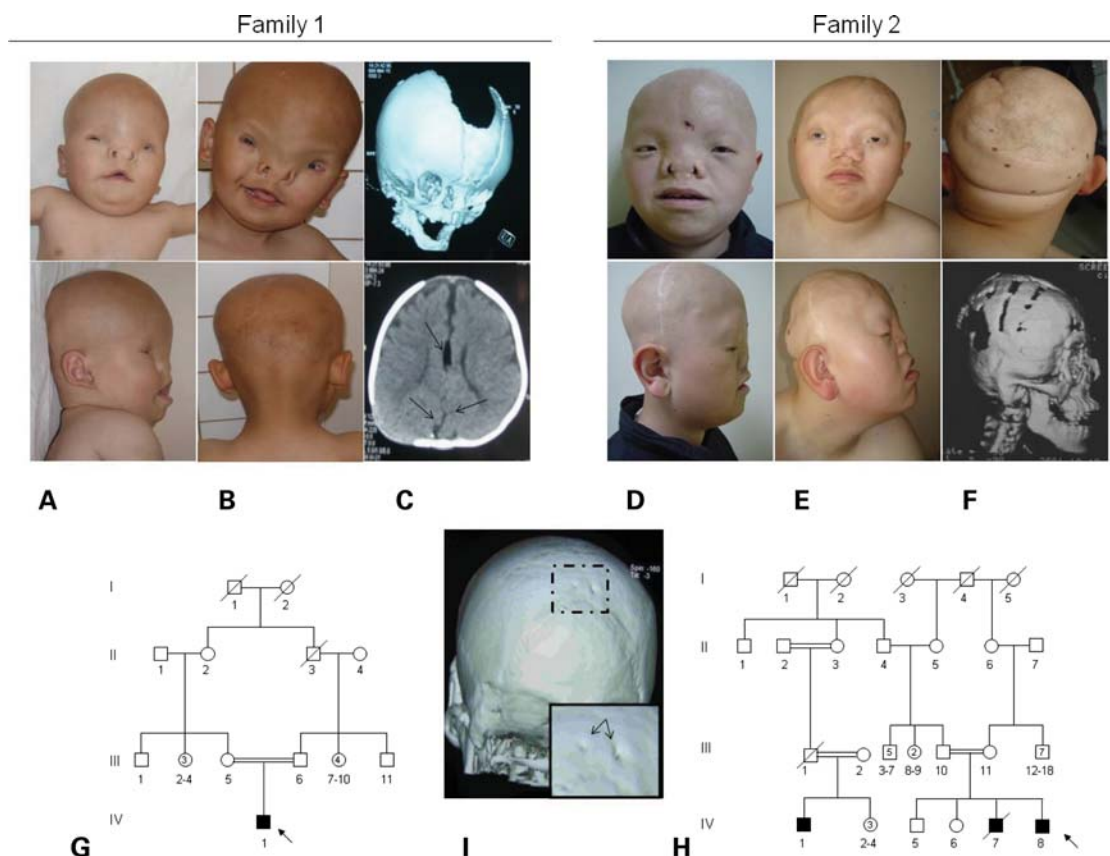


**Figure 1.** Clinical presentation of affected cases. (A) Frontal and side views of the first case (IV-1, Family 1) at 1 year of age showing total alopecia, brachycephaly, prominent forehead, marked hypertelorism, telecanthi, blepharophimosis, microphthalmia, broad nasal bridge and ridge, bifid and depressed nasal tip, broad columella, anteverted nares, notched alae nasi, broad philtrum and low-set ears with large lobules that were uptilted. Side view of the case demonstrates brachydactyly due to coronal suture synostosis. (B) The pictures of the same patient at the age of 3. Back view of the case demonstrates sparse, fine hair. (C) Upper part—3D cranial CT scan of the same patient demonstrating large calvarial defect, increased distance between the orbits, aplasia of ethmoid and nasal bones and underdevelopment of the maxillary bones. (C) Bottom part—non-enhanced CT scan demonstrating non-convergence of the lateral ventricles due to the absence of the corpus callosum, midline mass compatible with lipoma and interdigitation of the gyri posteriorly. (D) Frontal and side views of the second case (IV-8, Family 2) with similar craniofacial findings at the age of 8. (E) The clinical pictures of IV-8 in Family 2 at the age of 19 prior to alar cleft reconstructive surgery. (F) Upper part—back view of the case showing sparse hair and number of naevi on the occipital region. Note the irregular shape of the calvarium due to large skull defects. (F) Bottom part—3D-CT scan at the age of 8 years demonstrating brachycephaly with large calvarial bone defect at posterior part of parietal bones and multiple bilateral osteotomies in parietal and frontal bones. Aplasia of nasal bones and maxillary hypoplasia was noted. (G) Pedigree of the Family 1. (H) Pedigree of the Family 2. Probands in each family are indicated by an arrow. (I) 3D-CT of one of the parents, (Family 1, III-6) showing small parietal foramina (arrowhead).

the 250K-SNP mapping array. The mean call rate ( $\pm$  SD) was  $90.71 \pm 2.39\%$  (range 86.57–92.64%). Affected individual IV-8 from Family 2 was chosen to construct genome-wide haplotypes. Haplotypes indicating homozygosity by descent were compared with identical homozygous haplotypes of affected individual IV-1 of Family 1 (<http://www.hemosoft.com/Genom/Pubs/Frontonasal/Kaysirili/index.htm>).

Since regions of autozygosity are expected to be large in children born to first cousin marriages (13), homozygous stretches that spanned  $>10$  cM ( $\sim 10$  Mb) were taken into account as significant. We observed a single long homozygote segment of 19.8 Mb in size between 43,059,474 and 62,876,042 bp on chromosome 11p11.2–q12.3. No additional overlapping homozygous haplotype stretches of the expected size were observed throughout the genome. A total of 301 known genes were located in the critical interval on 11p11.2–q12.3 region. The human ortholog of mouse

aristal-less-like homeobox 4 gene, *ALX4*, was selected as a candidate gene because mice carrying homozygous mutation in *Alx4* exhibit craniofacial defects and dorsal alopecia (14,15), and because heterozygous *ALX4* loss-of-function mutations in humans cause skull defects, i.e. parietal foramina (FPM; OMIM 168500) (16–18). Sequencing allowed identification of homozygous nonsense mutation (c.793C $\rightarrow$ T) in exon 3 of *ALX4* in both available patients (Fig. 2A). This mutation is predicted to result in a premature stop codon (p.R265X) thereby removing 146 amino acids of the protein. The truncation affects part of the highly conserved homeodomain and the C-terminal paired tail domain (Fig. 2B). Using restriction digestion analysis with *AclI*, the homozygous state of the mutation was independently confirmed in both affected individuals as well as heterozygosity in the parents in both families (Fig. 2C). The c.793C $\rightarrow$ T mutation was not detected in 50 unaffected healthy Turkish controls.

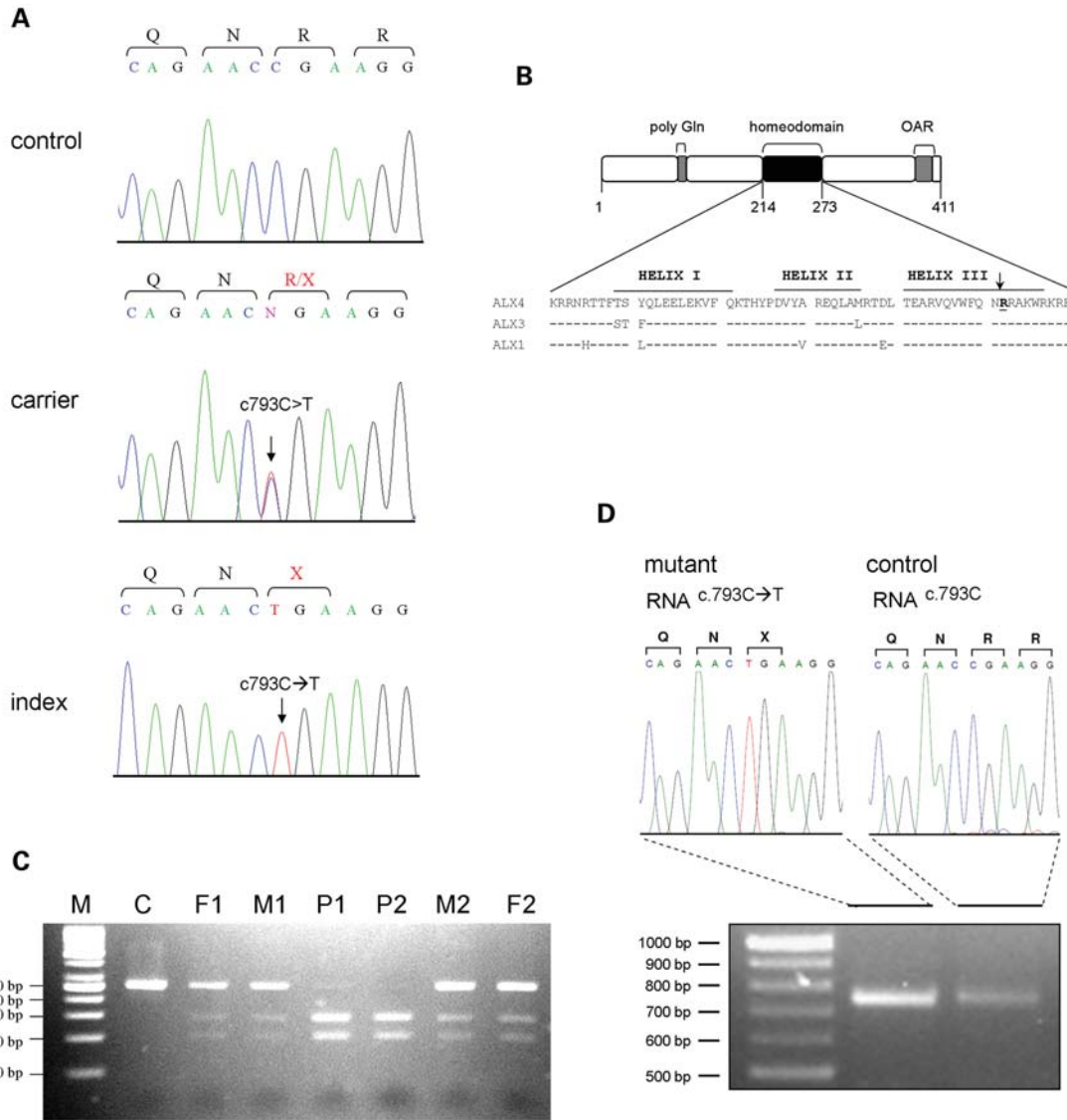


**Figure 2.** Identification of the novel homozygous nonsense mutation in the highly conserved homeodomain of *ALX4*. (A) Sequence chromatograms of an unaffected control individual (wild-type), a parent (carrier) and an affected case (mutant) showing c.793C→T nonsense mutation in heterozygous and homozygous state, respectively. (B) Schematic representation of the position of domains and motifs of *ALX4* protein obtained from uniprot database (<http://www.uniprot.org/uniprot/Q9H161>). The protein consists of poly-glutamine (poly-Gln) repeats, the homeodomain and aristaless-like domain (OAR). The arrowhead represents the position of the mutation, R265X within the homeodomain of *ALX4*, compared with other *ALX* family proteins (human *ALX3* and *ALX1*). (C) Confirmatory restriction digestion results of c.793C→T mutation in family members. No *AclI* site is present in the amplicons of homozygous wild-type control individual in contrast to the complete or partial digestion in patients and parents, respectively. (D) RT–PCR results showing the presence of *ALX4* mRNA in osteoblast cell lines of affected individual IV-8 of Family 2 and a control osteoblast cell line. The sequence chromatograms above show the presence of the of the c.793C→T nonsense mutation in the patient transcripts, whereas control mRNA shows normal wild-type sequence.

**RNA stability of the *ALX4* mutation**

RT–PCRs in a fibroblast culture and osteoblast cell line of an affected individual amplified a fragment that included *ALX4* exons 2, 3 and part of exon 4, and sequencing of this fragment confirmed the presence of c.793C→T mutation in these transcripts (Fig. 2D). The *ALX4* mutation was not present in an RT–PCR of a control osteoblast culture. This indicated that the mutated *ALX4* transcript was stable and not obviously affected by NMD. An effort to test the stability of the *ALX4* mutant protein using three different *ALX4* antibodies in western blot analysis in combination with immunoprecipitation

failed to detect both truncated and wild-type *ALX4* protein in patient and control osteoblasts, respectively, possibly due to lack of specificity of the antibody. Thus, it remains at present unclear whether the stop codon results in the expression of a stable or unstable mutant protein in native cells. Overexpression of the *ALX4* mutation in HEK293T cells resulted in a stable truncated protein as observed in western blot analysis (data not shown). We also tested if the localization mutant *ALX4* protein overexpressed in COS7 cells might be disturbed. Indeed, we could show that in contrast to the exclusive nuclear localization of wt *ALX4*,

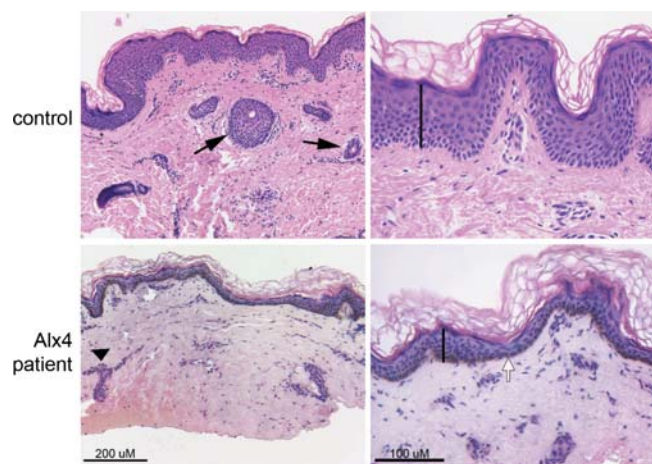


**Figure 3.** Hypomorphic epidermis and aberrant hair follicles in the skin of an *ALX4* patient. Paraffin sections of age and body site-matched control and *ALX4* patient skin were stained with hematoxylin/eosin to examine skin structure. Note the thin epidermis (compare length of black line drawn on epidermis in lower left panel to length of black line in upper left panel) in the *ALX4* patient. The hair follicle structures in the *ALX4* patient have an aberrant appearance (e.g. black arrowhead, lower right panel) when compared with control follicles (e.g. upper left panel, black arrows). The strong pigment staining (brown color, white arrow in lower left panel) in the basal layer in the *ALX4* patient should be noted. Right panels: scale bar is 200  $\mu\text{m}$ , left panels: scale bar is 100  $\mu\text{m}$ .

mutant protein is located in the cytoplasm not entering the nucleus (Supplementary Material, Fig. S1). Therefore, even if in native cells, the mutation results in a stable truncated protein, this protein is mislocalized to the cytoplasm causing complete loss-of-function.

### *ALX4* mutation affects epidermal differentiation

*Alx4* has been described to be primarily expressed in mesenchyme (19,20). Surprisingly, histochemical analysis of a skin section of the index patient of Family 1 revealed no obvious strong differences in the dermis, but instead, showed major changes in the epidermal compartment of the skin. The interfollicular epidermis was hypomorphic with less suprabasal layers when compared with an age and site-matched control individual (Fig. 3). In addition, although granules are present in the stratum granulosum (granular layer) of the epidermis, these were focally distributed and strongly reduced. In contrast, no obvious strong differences could be observed in the histology of the dermis of the patient.

To further examine if the hypomorphic skin and altered appearance of the granular layer correlated with overall changes in the interfollicular epidermal differentiation, we analyzed the expression of several differentiation markers that identify each of the viable layers of the epidermis, the basal, spinous and the granular layers (Fig. 4A). Whereas the control age and site-matched skin showed a strong positive staining in the basal layer for the basal layer marker keratin 14 (K14), this staining was strongly reduced but not absent in the patient, as shown by overexposure. More importantly, staining was confined to the basal layer. Similarly, staining for filaggrin, a marker for the granular layer, showed a strongly

reduced but not absent staining in the granular layer of the epidermis of the *ALX4* patient when compared with control epidermis. However, staining for keratin 10 (K10), a marker for the spinous layers, was not detectable in the *ALX4* affected skin, whereas control showed a strongly positive staining for all suprabasal layers, as expected. In addition, staining of the control for the keratin 15 (K15) showed patches of positive cells in the basal layer, as has been described previously, but this staining was absent in the *ALX4* patient basal layer (Fig. 4A). Together, these results indicate an impaired interfollicular epidermal differentiation.

Hair follicle-like structures were still observed by H&E staining, even though the patient lacked almost all body hair. However, the appearance of these structures was altered varying from only mildly altered structures to structures that appeared merely as a condensation of cells (Figs 3 and 4B). Nevertheless, these structures are positive for K14, indicating that they are derived from the interfollicular epidermis (Fig. 4B). However, K14 staining was inappropriately expressed in the inner layers of the most normal appearing hair follicle structure (Fig. 4B), indicating that also in this structure regular hair follicle differentiation is perturbed. No K15 staining, a hair follicle stem cell marker, could be detected in any of the hair follicle-like structures (Fig. 4C). In addition, staining for another stem cell marker,  $\beta$ 1 integrin, was also strongly reduced to absent in hair follicles of the *Alx4* patient when compared with control (Supplementary Material, Fig. S2).

### Alterations in junctional beta-catenin expression

*ALX4* was reported to be a mesenchymal factor that may interact with and affect Wnt/ $\beta$ -catenin signaling (21). Since this pathway is crucial for hair follicle development and cycling, we examined whether the *ALX4* mutation caused alterations in  $\beta$ -catenin localization. Control staining showed a strong staining for  $\beta$ -catenin at sites of intercellular contacts in both, interfollicular epidermis and hair follicle (Fig. 5). This result was expected since  $\beta$ -catenin is also an important component of the cadherin intercellular adhesion complex, which localizes to membranes at sites of cell–cell contacts. In addition, no obvious nuclear staining was detected in the interfollicular epidermis in control skin. Surprisingly, a strong reduction in intercellular  $\beta$ -catenin staining was observed in hair follicles and interfollicular epidermis of the *ALX4* patient, suggesting a reduction in cadherin mediated adhesion. This was not obviously accompanied by increased nuclear staining.

## DISCUSSION

Here we report a novel malformation syndrome of the frontonasal dysplasia spectrum manifesting severe and early craniofacial developmental delay, and associated with total alopecia and genital abnormalities. Although the presented phenotype, alopecia associated with frontonasal dysplasia, is new and to the best of our knowledge has not yet been described, it does share overlapping features with other previously reported frontonasal malformation syndromes. There is a great variability in

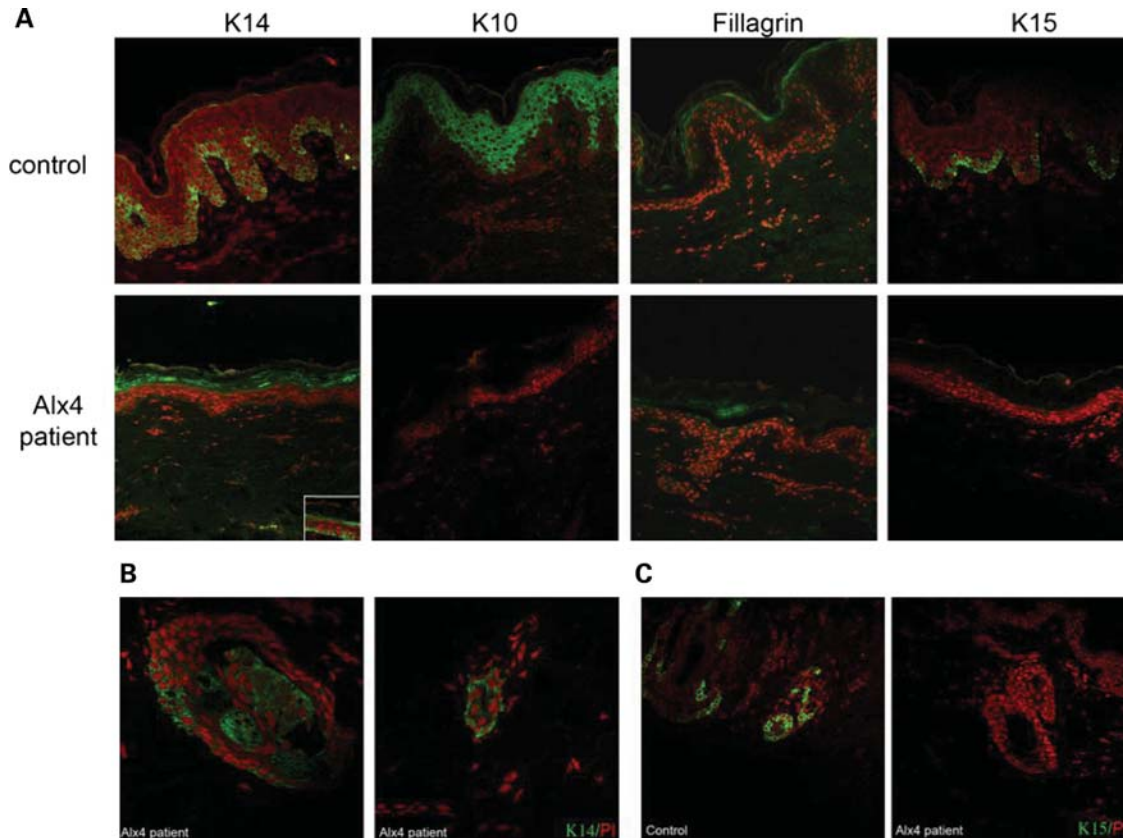


**Figure 4.** Impaired interfollicular epidermal and hair follicle differentiation. (A) Paraffin sections of age and body site-matched control and *ALX4* patient skin were stained with antibodies directed against the indicated markers (green). Nuclei were counterstained with propidium iodide (red). K14 was strongly reduced but upon prolonged exposure a signal was still observed in the correct layer (insert, lower left panel). Filaggrin expression was also reduced but still expressed in the appropriate layer in the patient carrying an *ALX4* mutation as for K14, whereas K10 and K5 were undetectable. (B) Paraffin sections of *ALX4* patient skin were stained for keratin 14 (K14, green) and propidium iodide (PI, red). The hair follicle structures still express K14, albeit is reduced, suggesting that these structures did originate from the interfollicular epidermis. (C) Reduced keratin 15 (K15) staining in hair follicles. Paraffin sections of control and *ALX4* patient skin were stained for K15 (green) and propidium iodide (PI, red) to counterstain nuclei.

the phenotypic expression of the frontonasal dysplasia spectrum, in which overlapping craniofacial malformations, including anterior cranium bifidum, various degrees of bifid nose, hypertelorism, median cleft, brachycephaly, can be associated with limb defects such as tibial hypoplasia/aplasia, preaxial polydactyly or cryptorchidism in some cases. In addition, central nervous system anomalies such as total/partial agenesis of corpus callosum or pericallosal lipoma have been frequently associated with some of these syndromes (8,22–25). Spectrum of craniorhiny (OMIM 123050) and craniorhiny-like phenotype with different modes of inheritance, showing brachycephaly associated with a nasal configuration strikingly similar to our cases, is another entity that should be considered in differential diagnosis (26–28). The combination of craniofacial, limb and brain anomalies is named as acromelic frontonasal dysostosis (AFND; OMIM 603671). Most affected males also have cryptorchidism in AFND (7,29). The clinical phenotype presented in this paper shows overlapping features with AFND, craniorhiny, craniofrontonasal dysplasia and cerebrofrontofacial syndrome. However, alopecia has not yet been described before in association with any of these syndromes. Also, the lack of limb malformations in our cases clearly distinguishes it from AFND.

The mode of inheritance of our *ALX4*-related FrontoNasal Dysplasia with Alopecia and Genital abnormality phenotype (short *ALX4*-related FNDAG) was autosomal recessive and we showed that a founder mutation in both families contributed to the etiology of this condition. This is the first description of a recessively inherited *ALX4* phenotype caused by a homozygous nonsense mutation. Previously, heterozygous *ALX4* missense, nonsense and frame-shift mutations leading to loss of protein function were identified in patients with parietal foramina (16–18,30). The father of Family 1 showed a comparable cranial defect observed by CT imaging. Our findings do support the observation that parietal foramina as a manifestation of heterozygous *ALX4* mutations has a reduced penetrance.

*ALX4* belongs to the family of aristaless-like homeobox genes, a distinct type of homeobox family characterized by a paired type homeodomain and a conserved C-terminal paired tail domain (31). Members of this gene family including *Alx1* (*Cart1*), *Alx3* and *Alx4* encode transcription factors that are expressed during embryogenesis in similar patterns in neural crest derived mesenchymal cells (31). Structural properties of paired class of homeodomain proteins (HD-proteins) are similar to other HD-protein families due to the presence of

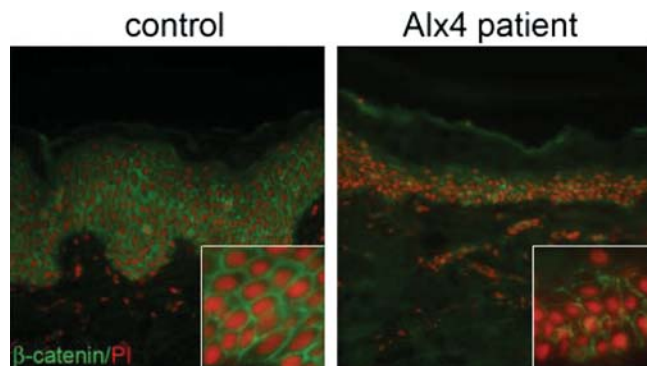


**Figure 5.** Strong reduction in adherens junction associated  $\beta$ -catenin. Paraffin sections of age and body site-matched control and *ALX4* patient skin were stained with a rabbit monoclonal against  $\beta$ -catenin (green). Nuclei were counterstained with propidium iodide (PI, red). Note the strongly reduced  $\beta$ -catenin at sites of cell–cell contacts.

a conserved 60 amino acid helix–turn–helix motif DNA binding domain (32). HD-proteins have a single DNA recognition motif in helix III, which binds major groove of target DNA. In addition, HD-proteins can target site specific P-elements (palindromic repeats of the sequence 5'-TAAT-3') and it has been demonstrated that amino acid residue 50 within the DNA recognition helix of the homeodomain mediates contacts with P elements (33). *ALX4* belongs to the group of Gln-50 paired homodomains (34). The homozygous p.R265X nonsense mutation causes a truncation of 146 C-terminal amino acids including part of the helix III of the homeodomain as well as the consensus sequence motif paired tail. This mutation corresponds to 52nd residue of the homeodomain and the key amino acid Gln at position 50, which mediates contact with the P elements of the target DNA, is predicted not to be disturbed. However, the recognition helix (helix III) is the most conserved part of HD-proteins and directly interacts with DNA major groove. Arginine residue at position 52 (Arg52) appears to be critical both for the conformational stability of the recognition helix and optimal DNA interactions with major groove (reviewed in 35). It was also experimentally shown that a C-terminal truncation of another HD-protein, LMX1B, exhibited a dramatically reduced transactivation in a reporter gene assay (36). These observations support that disruption of the helix III and additional complete loss of paired tail motif most likely cause loss of *ALX4* protein function. We could show that the mutant *ALX4* RNA is stable, but could not provide a definite answer to the question, if truncated protein is stable as well. But we showed that overexpressed truncated *ALX4* protein is mislocalized to the cytoplasm and this finding strongly supports the view that p.R265X is a loss-of-function mutation.

*Alx4* expression is mainly restricted to mesenchymal condensations during the development of several tissues and organs, such as bones, limbs, hair, whiskers, teeth and mammary tissues, and this development is largely dependent on epithelial–mesenchymal interactions (20). In heterozygote *Alx4* mutant mice, preaxial polydactyly was present in hindlimbs (37,38). Interestingly, homozygous *Alx4* mutant mice share several phenotypic characteristics with the *ALX4*

patients presented in this study. Mice exhibit reduced size of parietal bones, localized, dorsal alopecia and genital anomalies (37). In contrast, whereas mice also show severe preaxial polydactyly of all four limbs, absence of the tibia, and ventral body wall weakness, these features were not observed in the human phenotype (14,15,37). Especially, the absence of limb anomalies in p.R265X homozygous patients was an unexpected finding suggesting the existence of overlapping or compensatory mechanisms by other factors in humans. It is important to note that an additive effect on impaired craniofacial development was observed in *Alx4/Alx3* double mutant mice, which showed a severe nasal clefting in addition to aggravated severe skull defects resembling the craniofacial phenotype in human *ALX4* homozygotes (39). Beyond the structural relation between *Alx3* and *Alx4*, both genes show a similar expression pattern and overlapping functions (39). Also the third protein highly related to *Alx3* and *Alx4*, *Cart1* (*Alx1*), is expressed in craniofacial regions and mutant *Cart1* mice have a cranial phenotype (40). As the murine *Alx4* gene is expressed in and plays a pivotal role for the developing craniofacial mesenchyme, the observed frontofacial dysplasia in our patients indicate a similar function during human craniofacial development and homozygous *ALX4* dysfunction in humans even leads to a more severe craniofacial phenotype. Furthermore, cerebral manifestations have not been described in mutant mice. It is important to note that, at the time of the submission of this manuscript, a craniorhiny-like phenotype, renamed as frontorhiny, was reported caused by homozygous *ALX3* mutations (41). Our data further supports that both *ALX3* and *ALX4* have similar function especially in craniofacial development in human. In this context, it is important to state that a compensating effect of *ALX1* and *ALX3* on the *ALX4* phenotype is absolutely possible.

A very interesting observation was the association of almost complete alopecia with homozygous *ALX4* dysfunction. The sparse hair that was observed showed a brittle and wavy appearance indicating impaired formation of these hairs. Such alopecia has not yet been observed in any of the previously described frontonasal dysplasia syndromes. Dorsal alopecia has also been reported in Strong's luxoid (1st) mice (37), indicating that the regulation of hair follicle differentiation is a conserved function of *Alx4*. Histochemical analysis did reveal the presence of hair follicle-like structures, which stained positive for K14, suggesting that mutant *Alx4* does not interfere with initial stages of hair follicle morphogenesis. Nevertheless, these hair follicles showed an abnormal, underdeveloped appearance, which might explain the observed alopecia. Moreover, markers for hair follicle stem cells, such as beta1 integrin or K15, were strongly reduced in these structures, thus indicating abnormal hair follicle formation and differentiation that may result in underdeveloped hair follicle structures.

Hair follicle development and maintenance depend on reciprocal signaling between the mesenchymal and epithelial skin compartments. Since *Alx4* is primarily expressed in mesenchymal condensations, this suggests that *Alx4* plays an important role in this mesenchymal–epithelial communication, perhaps by affecting signal pathways like sonic hedgehog or *Wnt*, which are important regulators of hair follicles. Using *Alx4*

mutant mice, a similar role was identified for *Alx4* in epithelial–mesenchymal interactions that regulate mammary epithelial morphogenesis (20). Increased beta-catenin signaling is often accompanied by increased cytoplasmic and nuclear staining as a result of stabilization of non-cadherin bound  $\beta$ -catenin. However, no obvious increase in either cytoplasmic or nuclear staining was observed in the epidermis of the *Alx4* patient. This might suggest that the *Alx4* mutation does not affect  $\beta$ -catenin signaling but this requires extensive further analysis to rule this out.

Interestingly, we did observe reduced  $\beta$ -catenin staining at intercellular contacts in both the interfollicular epidermis and the hair follicle, suggesting a reduction in the number of that classical cadherin-based adherens junctions (42). This might also contribute to the observed alopecia since loss of E-cadherin in the epidermis of mice results in hair loss (43,44). Together, the results presented here in combination with the mouse data strongly indicate an important function for *Alx4* in hair follicle development.

Our initial histochemical analysis of the skin not only indicated hair follicle defects but also showed a hypomorphic epidermis in association with an overall strong reduction in interfollicular epidermal differentiation markers such as K14 and K10. Although this has so far not been observed in the Strong's luxoid mice, this may require more detailed analysis of newborn mice since the adult mouse epidermis is much thinner than its human counterpart, thus making it more difficult to observe obvious differences. These results also imply a function for *Alx4* in the regulation of the interfollicular epidermis. Even though *Alx4* is a mesenchymal factor, we were unable to observe any major changes in the dermis of the patient, although additional analyses need to be performed in the future to exclude or show more subtle changes in the dermis.

In summary, we show that the homozygous *c.793C*→*T* nonsense mutation in the *ALX4* gene cause a new and distinct phenotype in the severe end of frontonasal dysplasia spectrum characterized by cranium bifidum, severe hypertelorism, nasal configuration mimicking craniorhiny nose, corpus callosum anomalies associated with lipoma causing mild mental retardation and furthermore with total alopecia and hypogonadism/criptorchidism. Histological and immunohistological analysis of patient's skin biopsy showed changes in the epidermal architecture, rudimentary hair follicles and significant changes in epidermal expression markers, indicating an essential role of *ALX4* also in skin structure and proper hair follicle development.

## MATERIALS AND METHODS

### Patients

Two Turkish families with in total four affected individuals were included in this study (Fig. 1A–H). Family 1 with a single-affected individual was ascertained by Medical Genetics Department, Istanbul Medical Faculty, Istanbul University. Family 2 with three affected individuals was independently identified at Hacettepe University, Ankara, by the Craniofacial Study Group. Detailed clinical and radiological evaluation, including 3D cranial CT and cranial MRI were

available for two patients. All parents underwent physical exams, and one parent (Family 1, III-6) who showed partial symptoms underwent 3D cranial CT. Written informed consent was taken from participating family members. Institutional ethical board approvals for the research project were obtained [Istanbul University Medical Faculty (Project number: 2008/1194) and Hacettepe University Medical Faculty (Project number: TBK 09/4-42)].

### Homozygosity mapping and mutation analysis

DNA from two affected cases and their parents were genotyped for single nucleotide polymorphisms (SNPs) with GeneChip Mapping 250K Array Set (Affymetrix, Santa Clara, CA, USA). Hacettepe University Microarray Facility was used to genotype the individuals; 250 ng of genomic DNA was digested by *NspI*, followed by adaptor ligation and PCR amplification with primers provided by manufacturer (Affymetrix). PCR amplification was then purified by using Qiagen MinElute 96 protocol (Qiagen Inc., Valencia, CA, USA), fragmented by DNase I, labeled with terminal deoxynucleotidyltransferase and hybridized to the Mapping 250K Nsp GeneChips. Genotype files (CHP files) were generated in Affymetrix GTYPE software and transferred to VIGENOS (Visual Genome Studio) Program, Hemosoft Inc., Ankara. The main objective of VIGENOS software is to visualize huge amount of genome data in a comprehensible visual screens. For a given set of SNP marker data, alleles are shown in colored boxes (or lines). The software is able to process Affymetrix CHP files directly from its original file. There is a flexible analysis ability of the software, which allows examining the marker array from a different viewpoint. During the analyses, the first process was filtering the markers according to the type of the analysis and removing the non-informative markers from the chip array set. The second process was coloring the marker data to visualize haplotype information. Coloring was performed using a color-mapping function defined in the analysis. In addition to the coloring functions, it was possible to define score functions for each marker to draw one-dimensional graphics columns (<http://www.hemosoft.com/Genom/Pubs/Frontonasal/Kayserili/index.htm>).

Primers were designed for the amplification of the four coding exons of the human *ALX4* gene (reference sequence from Ensembl: ENSG0000052850). All sequencing primers used in this study are included in Supplementary Material, Table S1. Sequence analysis was performed using BigDye Terminator Cycle Sequencing Kit (Applied Biosystems, Foster City, CA, USA) on an ABI 310 Automatic Sequencer (Applied Biosystems). The identified *c.793C*→*T* mutation in exon 3 created a restriction site for the enzyme *AclI*. Family members and 50 healthy controls were genotyped for the presence of *c.793C*→*T* using a restriction digestion analysis with *AclI*.

### RT-PCR and western blotting

Total RNA from primary fibroblast cell culture was obtained from the index patient of Family 1, and a primary osteoblast cell culture from the index patient of Family 2 was obtained

from the nasal region during reconstructive surgery. In addition, total RNA was obtained from a normal control fibroblast cell culture and a control osteoblast cell culture. One microgram of total RNA was reverse transcribed using RevertAid™ First Strand cDNA Synthesis Kit (Fermentas GmbH, Germany). cDNA was amplified using cDNA specific primers of *ALX4* (Supplementary Material, Table S1). PCR conditions were 94°C for 5 min as initial denaturation followed by two cycles of 94°C for 30 s, 64°C for 30 s and 72°C for 1 min, two cycles of 94°C for 30 s, 62°C for 30 s and 72°C for 1 min, two cycles of 94°C for 30 s, 60°C for 30 s and 72°C for 1 min and 30 cycles of 94°C for 30 s, 50°C for 30 s and 72°C for 1 min, finally 72°C for 5 min as final extension. Total protein from primary osteoblast cell lines established from patient and a control cell lines was isolated incubating in ice-cold RIPA buffer [1% NP-40, 10 mM Tris at pH 8.0, 150 mM NaCl, 1 mM EDTA and protease inhibitors P 2714 (Sigma-Aldrich, St Louis, MO, USA)]. Protein concentration of extracts was determined by BCA Protein Assay Kit (Pierce Protein Research Products, Thermo Fischer Scientific, Rockford, IL, USA), and 25 µg of total protein from each sample was separated by 4–12% SDS-PAGE and blotted on to nitrocellulose membrane (Invitrogen GmbH, Germany). Protein detection was performed using an anti-*ALX4* polyclonal antibody against the N terminus of *ALX4* (N-12) (Santa Cruz Biotechnology Inc., Santa Cruz, CA, USA), and peroxidase conjugated anti-goat IgG (Jackson ImmunoResearch Laboratories Inc., West Grove, PA, USA). Blots were developed using an enhanced chemiluminescence system, ECL Plus (Amersham, UK) followed by exposure on an autoradiographic film.

### Immunofluorescence stainings

Cos7 cells grown on coverslips were transiently transfected with expression constructs for HA-tagged wild-type or mutant *Alx4*. 24 h after transfection cells were washed with PBS, fixed with 4% paraformaldehyde for 15 min and permeabilized with 0.5% Triton X-100 for 10 min. Slides were incubated with HA rat monoclonal antibodies (Roche Diagnostics GmbH, Germany), followed by incubation with FITC-conjugated goat-anti-rat IgG (Santa Cruz Biotechnology Inc.). Cells were counterstained with DAPI for 1 min, mounted and viewed with a Zeiss Axioplan2 fluorescence microscope using a ×100 objective.

### Histology and immunohistochemistry

Skin biopsies were obtained from the antecubital region of the index patient in Family 1. Samples were fixed in 4% PFA and embedded in paraffin. A skin biopsy of an unaffected age-matched individual was obtained as control. Paraffin sections were stained with hematoxylin/eosin. Immunohistochemistry was performed on paraffin sections using polyclonal antibodies against K14, K10, fillagrin (Covance Inc., New Jersey, USA) K15 and a rabbit monoclonal antibody to β-catenin (Epitomics Inc., Burlingame, CA, USA). Secondary antibodies were coupled to Alexa 488 (Molecular Probes, Oregon, USA) or Cy3 (Jackson Laboratories, Maine, USA). Nuclei were counterstained using propidium iodide. Images

were obtained using either a Nikon Eclipse 800 microscope equipped with a DXM1200 digital camera or a Leica TCS confocal laser microscope.

### SUPPLEMENTARY MATERIAL

Supplementary Material is available at *HMG* online.

### ACKNOWLEDGEMENT

We are grateful to the families for their participation in the study. We thank to Hacettepe University Craniofacial Surgery Study Group members: Yucel Erk and Aycan Kayikcioglu (Plastic and Reconstructive Surgery), Kemal Benli (Neurosurgery), Aysenur Cila (Radiology), Tulin Taner and Ilken Kocadereli (Orthodonty) for their evaluation of frontonasal malformation cases in the registry; Serra Sencer and Ensar Yekeler from radiology Department of Istanbul Medical Faculty for evaluation of 3D-CT scans and cranial MRI.

*Conflict of Interest statement.* None declared.

### FUNDING

This work was supported by the Scientific and Technology Research Council of Turkey (TUBITAK) [grant numbers 108S420 (to N.A.A.) and 108S418 (to H.K.)]; and German Federal Ministry of Education and Research Grants [grant numbers [01GM0801 (to B.W.) and SFB829 (to C.M.N. and I.H.)]. Responsibility for the contents rests with authors. Overall consortium (CRANIRARE) was supported by the European Research Area Network ‘E-RARE’ [Project number R07197KS].

### REFERENCES

- Carlson, B.M. (1994) *Human Embryology and Developmental Biology*. Mosby-Year Book Inc., Von Hoffmann Press, St Louis, Missouri.
- Richman, J.M. and Tickle, C. (1992) Epithelial–mesenchymal interactions in the outgrowth of the limb buds and facial primordial in chick embryos. *Dev. Biol.*, **54**, 299–308.
- Helms, J.A. and Schneider, R.A. (2003) Cranial skeletal biology. *Nature*, **423**, 326–330.
- Sedano, H.O., Cohen, M.M. Jr, Jirasek, J. and Gorlin, R.J. (1970) Frontonasal dysplasia. *J. Pediatr.*, **76**, 906–913.
- Sedano, H.O. and Gorlin, R.J. (1988) Frontonasal malformation as a field defect and in syndromic associations. *Oral. Surg. Oral. Med. Oral. Path.*, **65**, 704–710.
- Guion-Almeida, M.L., Richieri-Costa, A., Saavedra, D. and Cohen, M.M. Jr (1996) Frontonasal dysplasia, analysis of 21 cases and literature review. *In. J. Oral. Maxillofac. Surg.*, **25**, 91–97.
- Slaney, S.F., Goodman, F.R., Eilers-Walsman, B.L.C., Hall, B.D., Williams, D.K., Young, I.D., Hayward, R.D., Jones, B.M., Christianson, A.L. and Winter, R.M. (1999) Acromelic frontonasal dysostosis. *Am. J. Med. Genet.*, **83**, 109–116.
- Guion-Almeida, M.L. and Richieri-Costa, A. (2001) Frontonasal dysplasia, macroblepharon, eyelid colobomas, ear anomalies, macrostomia, mental retardation and CNS structural anomalies, defining the phenotype. *Clin. Dysmorphol.*, **10**, 81–86.
- Twigg, S.R.F., Kan, R., Babbs, C., Bochukova, E.G., Robertson, S.P., Wall, S.A., Morriss-Kay, G.M. and Wilkie, A.O.M. (2004) Mutations of ephrin-B1 (EFNB1), a marker of tissue boundary formation, cause craniofrontonasal syndrome. *Proc. Natl Acad. Sci. USA*, **101**, 8652–8657.

10. Wieland, I., Jakubiczka, S., Muschke, P., Cohen, M., Thiele, H., Gerlach, K.L., Adams, R.H. and Wieacker, P. (2004) Mutations of the ephrin-B1 gene cause craniofrontonasal syndrome. *Am. J. Hum. Genet.*, **74**, 1209–1215.
11. Tessier, P. (1976) Anatomical classification facial, cranio-facial and latero-facial clefts. *J. Maxillofac. Surg.*, **4**, 69–92.
12. Kawamoto, H.K. Jr (1976) The kaleidoscopic world of rare craniofacial clefts, order out of chaos (Tessier classification). *Clin. Plast. Surg.*, **3**, 529–572.
13. Lander, E.S. and Botstein, D. (1987) Homozygosity mapping, a way to map human recessive traits with the DNA of inbred children. *Science*, **236**, 1567–1570.
14. Qu, S., Niswender, K.D., Ji, Q., van der Meer, R., Keeney, D., Magnuson, M.A. and Wisdom, R. (1997) Polydactyly and ectopic ZPA formation in Alx-4 mutant mice. *Development*, **124**, 3999–4008.
15. Qu, S., Tucker, S.C., Ehrlich, J.S., Levorse, J.M., Flaherty, L.A., Wisdom, R. and Vogt, T.F. (1998) Mutations in mouse aristaless-like4 cause Strong's luxoid polydactyly. *Development*, **125**, 2711–2721.
16. Wuyts, W., Cleiren, E., Homfray, T., Rasore-Quartino, A., Vanhoenacker, F. and Van Hul, W. (2000) The ALX4 homeobox gene is mutated in patients with ossification defects of the skull (foramina parietalia permagna, OMIM 168500). *J. Med. Genet.*, **37**, 916–920.
17. Mavrogiannis, L.A., Antonopoulou, I., Baxova, A., Kutilek, S., Kim, C.A., Sugayama, S.M., Salamanca, A., Wall, S.A., Morriss-Kay, G.M. and Wilkie, A.O.M. (2001) Haploinsufficiency of the human homeobox gene ALX4 causes skull ossification defects. *Nat. Genet.*, **27**, 17–18.
18. Mavrogiannis, L.A., Taylor, I.B., Davies, S.J., Ramos, F.J., Olivares, J.L. and Wilkie, A.O.M. (2006) Enlarged parietal foramina caused by mutations in the homeobox genes ALX4 and MSX2, from genotype to phenotype. *Eur. J. Hum. Genet.*, **14**, 151–158.
19. Qu, S., Li, L. and Wisdom, R. (1997) Alx-4, cDNA cloning and characterization of a novel paired-type homeodomain protein. *Gene*, **203**, 217–223.
20. Hudson, R., Taniguchi-Sidle, A., Boras, K., Wiggan, O. and Hamel, P.A. (1998) Alx-4, a transcriptional activator whose expression is restricted to sites of epithelial–mesenchymal interactions. *Dev. Dyn.*, **213**, 159–169.
21. Boras, K. and Hamel, P.A. (2002) Alx4 binding to LEF-1 regulates N-CAM promoter activity. *J. Biol. Chem.*, **277**, 1120–1127.
22. Toriello, H.V., Radecki, L.L., Sharda, J., Looyenga, D. and Mann, R. (1986) Frontonasal 'dysplasia,' cerebral anomalies, and polydactyly, report of a new syndrome and discussion from a developmental field perspective. *Am. J. Med. Genet. Suppl.*, **2**, 89–96.
23. Pai, G.S., Levkoff, A.H. and Leithiser, R.E. Jr (1987) Median cleft of the upper lip associated with lipomas of the central nervous system and cutaneous polyps. *Am. J. Med. Genet.*, **26**, 921–924.
24. Lees, M.M., Hodgkins, P., Reardon, W., Taylor, D., Stanhope, R., Jones, B., Hayward, R., Hockley, A.D., Baraitser, M. and Winter, R.M. (1998) Frontonasal dysplasia with optic disc anomalies and other midline craniofacial defects, a report of six cases. *Clin. Dysmorphol.*, **7**, 157–162.
25. Masuno, M., Imaizumi, K., Aida, N., Nishimura, G., Kimura, J. and Kuroki, Y. (2000) Frontonasal dysplasia, macroblepharon, eyelid colobomas, ear anomalies, macrostomia, mental retardation, and CNS structural anomalies, another observation. *Clin. Dysmorphol.*, **9**, 59–60.
26. Tange, I. (1997) A peculiar malformation of the upper lip, Report of six cases. *Cleft Palate Craniofac. J.*, **34**, 73–78.
27. Mindikoglu, A.N., Partington, M.W. and Cohen, M.M. Jr (1991) Noses nobody knows for real-rhiny and craniorhiny. *Am. J. Med. Genet.*, **40**, 250–251.
28. Lees, M.M., Kangesu, L., Hall, P. and Hennekam, R.C. (2007) Two siblings with an unusual nasal malformation, Further instances of craniorhiny? *Am. J. Med. Genet. A.*, **143A**, 3290–3294.
29. Hing, A.V., Syed, N. and Cunningham, M.L. (2004) Familial acromelic frontonasal dysostosis, autosomal dominant inheritance with reduced penetrance. *Am. J. Med. Genet. A.*, **128A**, 374–382.
30. Valente, M., Valente, K.D., Sugayama, S.S. and Kim, C.A. (2004) Malformation of cortical and vascular development in one family with parietal foramina determined by an ALX4 homeobox gene mutation. *Am. J. Neuroradiol.*, **25**, 1836–1839.
31. Meijlink, F., Beverdam, A., Brouwer, A., Oosterveen, T.C. and Berge, D.T. (1999) Vertebrate aristaless-related genes. *Int. J. Dev. Biol.*, **43**, 651–663.
32. Gehring, W.J., Qian, Y.Q., Billeter, M., Furukubo-Tokunaga, K., Schier, A.F., Resendez-Perez, D., Affolter, M., Otting, G. and Wüthrich, K. (1994) Homeodomain-DNA recognition. *Cell*, **78**, 211–223.
33. Tucker, S.C. and Wisdom, R. (1999) Site-specific heterodimerization by paired class homeodomain proteins mediates selective transcriptional responses. *J. Biol. Chem.*, **274**, 32325–32332.
34. Wilson, D., Sheng, G., Lecuit, T., Dostatni, N. and Desplan, C. (1993) Cooperative dimerization of paired class homeodomains on DNA. *Genes Dev.*, **7**, 2120–2134.
35. Chi, Y.I. (2005) Homeodomain revisited. A lesson from disease-causing mutations. *Hum. Genet.*, **116**, 433–444.
36. Dreyer, S.D., Morello, R., German, M.S., Zabel, B., Winterpacht, A., Lunstrum, G.P., Horton, W.A., Oberg, K.C. and Lee, B. (2000) LMX1B transactivation and expression in nail–patella syndrome. LMX1B transactivation and expression in nail–patella syndrome. *Hum. Mol. Genet.*, **9**, 1067–1074.
37. Forsthoefel, P.F., Fritts, M.L. and Hatznbeler, L.J. (1966) The origin and development of alopecia in mice homozygous for Strong's luxoid gene. *J. Morphol.*, **118**, 565–580.
38. Takahashi, M., Tamura, K., Büscher, D., Masuya, H., Yonei-Tamura, S., Matsumoto, K., Naitoh-Matsuo, M., Takeuchi, J., Ogura, K., Shiroishi, T. et al. (1998) The role of Alx-4 in the establishment of anteroposterior polarity during vertebrate limb development. *Development*, **125**, 4417–4425.
39. Beverdam, A., Brouwer, A., Reijnen, M., Korving, J. and Meijlink, F. (2001) Severe nasal clefting and abnormal embryonic apoptosis in Alx3/Alx4 double mutant mice. *Development*, **128**, 3975–3986.
40. Ettensohn, C.A., Illies, M.R., Oliveri, P. and De Jong, D.L. (2003) Alx1, a member of the Cart1/Alx3/Alx4 subfamily of Paired-class homeodomain proteins, is an essential component of the gene network controlling skeletogenic fate specification in the sea urchin embryo. *Development*, **130**, 2917–2928.
41. Twigg, S.R.F., Versnel, S.L., Nürnberg, G., Lees, M.M., Bhat, M., Hammond, P., Hennekam, R.C.M., Hooeboom, A.J.M., Hurst, J.A., Johnson, D. et al. (2009) Frontorhiny, a distinctive presentation of frontonasal dysplasia caused by recessive mutations in the ALX3 homeobox gene. *Am. J. Hum. Genet.*, **84**, 698–705.
42. Niessen, C.M. (2007) Tight junctions/adherens junctions, basic structure and function. *J. Invest. Dermatol.*, **127**, 2525–2532.
43. Young, P., Boussadia, O., Halfter, H., Grose, R., Berger, P., Leone, D.P., Robenek, H., Charnay, P., Kemler, R. and Suter, U. (2003) E-cadherin controls adherens junctions in the epidermis and the renewal of hair follicles. *EMBO J.*, **22**, 5723–5733.
44. Tinkle, C.L., Lechler, T., Pasolli, H.A. and Fuchs, E. (2004) Conditional targeting of E-cadherin in skin, insights into hyperproliferative and degenerative responses. *Proc. Natl Acad. Sci. USA*, **101**, 552–557.